Channel Power Gain Estimation for Terahertz Vehicle-to-infrastructure Networks

Zheng Lin, Lifeng Wang, Jie Ding, Bo Tan, and Shi Jin

***Abstract*—The use of terahertz (THz) frequencies has been recommended to achieve high-speed and ultra-low latency transmissions. Although there exist very large bandwidths in the THz frequency bands, THz channels are significantly dynamic and complicated, which is challenging for channel estimation. To improve the energy efficiency of wireless networks, THz channel power gains need to be precisely evaluated for determining optimal THz transmission frequencies and power control. Therefore, this work presents a novel conditional generative adversarial networks (GAN) based channel power gain estimation solution in the THz vehicle-to-infrastructure (V2I) networks with leaky-wave antennas, where the THz frequency has a big effect on the antenna gain, path loss and atmospheric attenuation. Simulation results confirm that our solution can accurately estimate the channel power gains versus the THz frequencies at a fast speed.**

***Index Terms*— Channel estimation, generative adversarial networks, terahertz vehicle-to-infrastructure.**

I. Introduction

Due to the availability of the abundant terahertz (THz) frequency bands, THz transmission is envisioned as the next-generation radio technology for wireless networks [1]. Compared to the sub-6GHz and millimeter wave (mmWave) enabled vehicle-to-infrastructure (V2I) systems, THz V2I has the potential to achieve ultra-low latency communication and ultra-high sensing accuracy [2].

It is known that narrow beams with large antenna gains are required to counteract the severe path losses in the higher frequencies. Therefore, 5G mmWave systems have already adopted large antenna arrays with high beam management complexities [3]. However, the implementations of conventional antenna arrays in THz systems are confronted with many challenges in terms of the hardware components/architecture [1], access latency [3, 4], link budget [4, 5] and path discovery [6] etc. As summarized in [3], there exist many key issues including inefficient beam sweeping and correspondence for beam management with large antenna arrays in the higher frequencies. In the THz V2I networks with high mobility, these issues will be more critical. Recent studies [4–7] suggest that new antenna solutions are encouraged to establish low-complexity and low-cost THz networks.

Channel estimation is essential for optimal transmission with efficient beam management and power control, however, it has to be redesigned in the THz systems since the traditional schemes with large phased arrays have many bottlenecks [3]. Moreover, the THz link with a very large number of antennas may have larger access latency [3, 4], which is detrimental for fast channel estimation, especially in mobile scenarios. Statistical and machine learning methods provide a data-driven manner to tackle this challenge, which have attracted much recent attention [8–10]. However, the traditional deep learning (DL) architectures have limited ability to generate the exact samples following the realistic channel distributions because of the data information loss in the successive layers of neural networks [11]. The generative adversarial networks (GAN) [12] aided channel estimation has attracted much attention, thanks to its capability of learning the underlying distribution from the data and producing samples statistically close to the underlying distribution. It is shown in [8] that the GAN based channel estimation method can achieve higher accuracy than some DL designs with deep convolutional neural networks or deep multilayer perceptrons. In [9], GAN is exploited to build the mapping function between the receive signal sequences and the channel covariance matrix. To develop the end-to-end wireless communication systems with DL, GAN is employed to characterize the channel effects in [13]. In [14], mmWave channel distribution is learned by using GAN. Therefore, GAN provides an appealing data-driven approach for channel estimation without requiring extensive training dataset.

Motivated by the aforementioned, we propose a new GAN based channel power gain estimation framework in the THz V2I network with leaky-wave antennas, which has not been conducted in the literature. Unlike the conventional wireless systems with phased arrays, the spatial-spectral coupling feature of the leaky-wave antenna can be exploited to design fast channel estimation. Such a novel THz antenna solution is efficient for achieving high-speed transmission in the dense THz networks [7]. The proposed estimation scheme overcomes the drawbacks of Doppler shift and conventional methods such as [15] that depend on state information in the prior time. Moreover, the significance of the designed GAN model is twofold: i) Different from the existing works such as [8, 9, 13, 14, 16] in which GAN model is designed by only splicing the conditional information vector and the noise vector once, we consider an additional cross layer splicing such that the conditional information vector is spliced twice. This operation can compensate the data information loss in

Manuscript received May 22, 2022; revised August 22, 2022 and September 21, 2022; accepted September 28, 2022. This work was supported in part by the National Key Research and Development Program under Grant 2021YFE0193300, and in part by Shanghai STCSM Program under Grant 22QA1401100. The work of Bo Tan was supported in part by the Academy of Finland under the project ACCESS (339519). The associate editor coordinating the review of this article and approving it for publication was M. Sepulcre. *(Corresponding author: Lifeng Wang.)*

Z. Lin, L. Wang and J. Ding are with the Department of Electrical Engineering, Fudan University, Shanghai, China (E-mail: {lifengwang, dingjie, ydxu}@fudan.edu.cn).

B. Tan is with the Faculty of Information Technology and Communication Sciences, Tampere University, Finland (E-mail: bo.tan@tuni.fi).

S. Jin is with National Mobile Communications Research Laboratory, Southeast University, Nanjing 210096, China (Email: jinshi@seu.edu.cn).

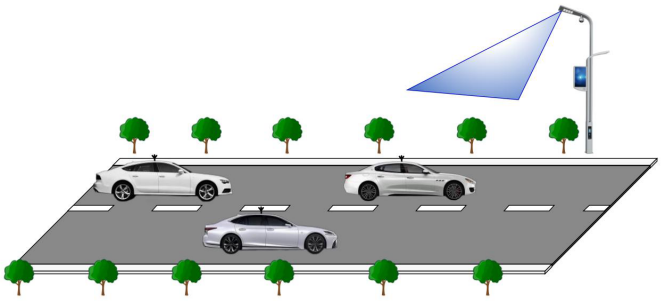

Fig. 1. An illustration of THz V2I network with leaky-wave antennas.

the successive layers of the neural networks and make the proposed GAN model generate samples more effectively; ii) Unlike existing GAN based methods with direct splicing, we extend the noise vector and the conditional information vector, to increase the richness of information and improve the efficiency of generating accurate samples. In the considered network, the received signal strengths (RSSs) are leveraged as the conditional information to train the proposed GAN model. With the help of the proposed GAN based solution, vehicles extract the channel power gain information from their received signal strengths (RSSs), and do not need any additional state information. The results confirm that the proposed solution can accurately predict the channel power gains of the corresponding frequencies and has a fast convergence speed.

The rest of this paper is organized as follows. The system model is described in Section II. The GAN-based channel estimation solution is designed in Section III. Section IV covers the simulation results. Finally, some concluding remarks are presented in Section V.

II. System Description

In the multi-vehicle THz downlink networks (illustrated by Fig. 1), each roadside unit (RSU) has one lowest transverse-electric (TE_1) mode leaky-wave antenna and each vehicle has one omnidirectional antenna. As mentioned by [17], the far-field radiation pattern of TE_1 mode leaky-wave antenna is given by

$$G\left(f,\varphi\right)=L\mathrm{sinc}\left[\left(-j\alpha-k_0\left(f\right)\cos\varphi+\beta\left(f\right)\right)\frac{L}{2}\right], \quad (1)$$

where f is the transmission frequency, φ is the propagation angle $(0<\varphi<90^o)$, L is the aperture length, $j=\sqrt{-1}$, α is the attenuation coefficient due to the power absorption in the structure, $k_0\left(f\right)=2\pi f/c$ with the speed of light c is the wavenumber of the free-space, $\beta\left(f\right)=k_0\left(f\right)\sqrt{1-\left(\frac{f_{\mathrm{co}}}{f}\right)^2}$ is the phase constant of the TE_1 mode based traveling wave, in which $f_{\mathrm{co}}=\frac{c}{2d}$ with the inter-plate distance d is the cutoff frequency. One of the key features for the leaky-wave antenna is that given a line-of-sight (LoS) direction φ of a vehicle, the frequency that has the maximum level of the radiation is calculated as [6]

$$f\left(\varphi\right)=\frac{f_{\mathrm{co}}}{\sin\varphi}. \quad (2)$$

It is indicated from (2) that the frequencies of interest around $f\left(\varphi\right)$ can be leveraged to achieve large radiated energy at the transmission direction φ.

Since each vehicle adopts the same mechanism, we focus on an arbitrary vehicle for notational convenience. The leaky-wave antenna's spatial-spectral coupling effects (signatures) enable that multiple vehicles can be identified by exploiting their unique link directions without a need for beam association. In practice, the reference signal can be formed as a moderate "THz rainbow" [6], i.e., signal components over different frequencies are radiated into the free-space at different directions due to the leaky-wave antenna's spatial-spectral coupling effect. Moreover, the reference signal only needs to consist of signal components in directions of interest (namely moderate propagation angle range that covers the desired direction from the RSU to a vehicle), thanks to the known prior link direction information. In addition, it has been confirmed in [7] that the THz network with leaky-wave antennas is noise-limited and co-channel interference is negligible. Therefore, the received reference signal at the center frequency f_n of the n-th subchannel for an arbitrary vehicle is written as

$$y_n\left(t\right)=\sqrt{p\tilde{G}\left(f_n,\varphi\left(t\right)\right)}\hbar_n z\left(t-\tau\right)e^{j2\pi f_n^{\mathrm{Doppler}}\left(t\right)t}+\varpi\left(t\right), \quad (3)$$

where p is the transmit power per subchannel, $\tilde{G}\left(f_n,\varphi\left(t\right)\right)=\xi G\left(f_n,\varphi\left(t\right)\right)$ is the effective antenna gain, here ξ is the radiation efficiency factor and can be easily obtained by measuring the effective antenna gain for a particular leaky-wave antenna structure, thus it can be known a priori [6], $\hbar_n$ is the THz channel coefficient at frequency f_n, $z\left(t\right)$ with $\mathbb{E}\{z\left(t\right)z^H\left(t\right)\}=1$ is the reference signal, τ is the propagation delay, $f_n^{\mathrm{Doppler}}\left(t\right)$ is the Doppler shift at time t, $\varpi\left(t\right)$ is the complex additive white Gaussian noise with zero mean and variance σ^2. In light of (3), the RSS observed at the vehicle is given by

$$\overline{y}_n=p\tilde{G}\left(f_n,\varphi\left(t\right)\right)\left|\hbar_n\right|^2+\overline{\varpi}, \quad (4)$$

where $\left|\hbar_n\right|^2$ is the channel power gain, $\overline{\varpi}\sim\exp\left(\lambda\right)$ is the exponential random variable with the parameter $\lambda=1/\sigma^2$. Our aim is to estimate the channel power gain $\left|\hbar_n\right|^2$ based on the observations $\overline{y}_n$. It should be noted that the level of effective antenna gain for a subchannel is unknown at the vehicle. The vehicles aim to estimate the channel power gains with the help of the proposed GAN based design, which is detailed in the following section.

III. Channel Estimation With Conditional Generative Adversarial Networks

GAN is introduced as an alternative approach to train generative models for addressing the difficulty of approximating many intractable probabilistic computations [12]. The rationale behind it is that raw data is leveraged to train two feed-forward neural networks, namely generator and discriminator: The generator $G(\cdot)$ captures the data underlying distribution; and the discriminator $D(\cdot)$ estimates the probability that a sample comes from the training data rather than $G(\cdot)$. Nevertheless, in this unconditional generative model, the generation of

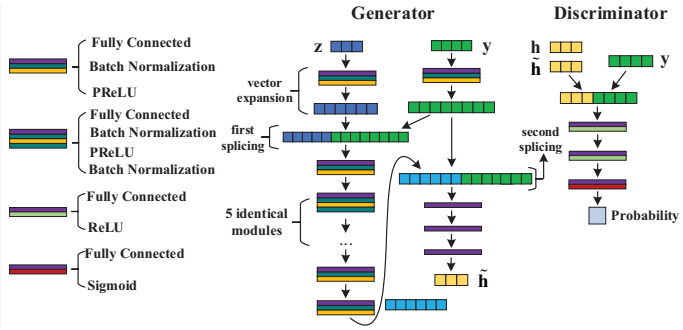

Fig. 2. Neural network architecture of the proposed GAN based solution.

data cannot be controlled. The conditional GAN [16] splices the conditional information vector and the noise vector as additional input layer to form a conditional generative model, so that the model can generate data under the guidance of the conditional information. Inspired by the GAN, we develop a novel conditional GAN based THz channel estimation solution, which can learn the complicated mapping function between the RSS and channel power gain.

As shown in Fig. 2, the input to the generator $G(\cdot)$ is the splicing of the noise vector $\mathbf{z}$ sampled from a priori distribution p_z (e.g. uniform distribution) and the conditional information vector $\mathbf{y}$. In the proposed design, the conditional information vector encompasses the center frequencies of the available subchannels and their corresponding RSSs (Vehicles cannot identify the channel power gain information belonging to which subchannel before processing). Therefore, the conditional information vector $\mathbf{y}$ can be written as

$$\mathbf{y} = [f_1, f_2, \cdots, f_n, \bar{y}_1, \bar{y}_2, \cdots, \bar{y}_n] \tag{5}$$

The objective of our proposed GAN based approach is to generate the estimated channel power gain vector $\tilde{\mathbf{h}}$ under the guidance of the conditional information vector $\mathbf{y}$. The estimated channel power gain vector $\tilde{\mathbf{h}}$ is given by

$$\tilde{\mathbf{h}} = \left[\left|\tilde{h}_1\right|^2, \left|\tilde{h}_2\right|^2, \cdots, \left|\tilde{h}_n\right|^2 \right]. \tag{6}$$

We first design the generator model. Different from direct splicing in existing GAN based methods such as [8, 9, 13, 14, 16], we extend the noise vector $\mathbf{z}$ and the conditional information vector $\mathbf{y}$, in order to increase the richness of information and improve the efficiency of generating accurate samples. The extended noise vector and conditional information vector are spliced as the additional input of the generator. The input splicing vector is then delivered into the multi-layer neural network structure, which includes three neural network layers, fully connected (FC) layer, batch normalization (BN) layer and PReLU activation layer. By increasing neural network depth, the activation function becomes more nonlinear, which leads to stronger fitting ability [18]. The main purpose of BN layer is to normalize the data and improve the gradient flowing through the network, so as to accelerate the convergence of the generative model. After multi-layer neural network processing, the output vector is spliced with the conditional information vector $\mathbf{y}$ for the second time and goes through three FC layers, to rescale the vector that has the same size as $\tilde{\mathbf{h}}$. The PReLU activation layer can retain more feature information in the shallow layer of the neural network, and has higher feature discrimination in the deep layer.

The input of the discriminator $D(\cdot)$ is either a real sample $\mathbf{h}$ from the targeted distribution p_{data}, or a generated sample $G(\mathbf{z}|\mathbf{y})$ (namely $\tilde{\mathbf{h}}$), and the output of the discriminator is a real value representing the probability that the input is sampled from the targeted distribution p_{data}. The input splicing vector flows through the three FC layers, and the activation layers are ReLU, ReLU, and Sigmoid, respectively.

In the training process, the generator $G(\cdot)$ attempts to generate fake samples, which can deceive the discriminator $D(\cdot)$. The discriminator $D(\cdot)$ learns to distinguish the fake samples generated by the generator $G(\cdot)$ and the real samples from the target distribution p_{data}. The training process converges when the Nash equilibrium of a minimax game between generator $G(\cdot)$ and discriminator $G(\cdot)$ is reached. The objective function of minimax game can be expressed as

$$\begin{aligned} \min_G \max_D \; V(D,G) = &\mathbb{E}_{\mathbf{h}\sim p_{data}(\mathbf{h})}\left[\log D(\mathbf{h}|\mathbf{y})\right] \\ &+\mathbb{E}_{\mathbf{z}\sim p_z(\mathbf{z})}\left[\log\left(1 - D(G(\mathbf{z}|\mathbf{y}))\right)\right], \end{aligned} \tag{7}$$

where $\mathbb{E}[\cdot]$ is the expectation operator. By training the proposed GAN model until convergence, the desired generator $G(\cdot)$ is obtained as our THz channel power gain estimator.

IV. Numerical Results

This section presents numerical results to confirm the efficiency of the proposed approach, which can well address the effects of path loss and atmospheric attenuation in the different THz frequencies. The values of the system parameters and the corresponding system computational complexity in the simulations are detailed as follows:

Channel model parameters: For the V2I THz channel measurement dataset, we adopt ITU's gaseous attenuation calculation model to generate real channel measurement data in the frequencies ranging from 100GHz to 400GHz [19], where the measured path losses and atmospheric attenuations with respect to the THz frequencies are provided. In the simulations, the propagation angle from the RSU to the vehicle is uniformly distributed, i.e., $\varphi \in U\left(0, \frac{\pi}{2}\right)$, the transmit power per channel is $p = 21.76$dBm, the communication distance is uniformly distributed within the coverage radius $r_{\max} = 30$m, the aperture length $L = 0.06$m, the leaky-wave antenna's attenuation coefficient is $\alpha = 90$rad/m, inter-plate distance $d = 1.5$mm, radiation efficiency factor $\xi = 1$ and the noise power is $\sigma^2 = -10$dBm. The simulation is conducted by using Python version 3.8 and PyTorch library 1.11.0.

GAN model parameters: Assume that the noise vector $\mathbf{z}$ length is M (usually set as a small integer) and the estimated channel power gain vector $\tilde{\mathbf{h}}$ length is N, therefore, the conditional information $\mathbf{y}$ length is $2N$. As shown in Fig. 2, for the generator, we first extend the lengths of noise vector and conditional information vector to 500 and 1000, respectively. After the first splicing, the vector length remains 1500 during the three-layer and five identical four-layers processes. Then the vector length is extended to 10000 and reduced to 1000 before the second splicing. At last, after going through three FC layers, the vector length is correspondingly reduced to

1500, 1000 and N. For the discriminator, we first extend the length of the splicing vector to 64, and then reduce the length to 32 and 1 in the final two FC layers, respectively. In addition, for each training, the training data batch fed into the model is 128; the generator $G(\cdot)$ and discriminator $D(\cdot)$ are trained 200 times in each epoch; the learning rates of the generator and discriminator are the same and set as 0.003. It is noted that the traditional GAN network [16] is employed as the benchmark, which has the identical layers and dimensions as the proposed GAN, and the difference of the proposed GAN network is that input vector expansion and twice splicing processes are introduced as illustrated in Fig. 2.

Computational complexity: The number of floating-point operations (FLOPs) is an important indicator to measure the computational complexity of neural networks. It is shown in [20] that the number of FLOPs for the FC layer is $(2I-1)O$, and the number of FLOPs for the BN layer is $2IO$, where I is the input dimensionality and O is the output dimensionality. The number of FLOPs for the PReLU and ReLU activation layers are the same as I, and the number of FLOPs for the Sigmoid activation layer is $4I$. As such, the number of FLOPs for the considered generator and the discriminator in the proposed GAN network are calculated as $5999N + 1000M + 3.399975 \times 10^8$ and $384N + 4160$. It is noted that for the traditional GAN network [16], the number of FLOPs of generator and discriminator are $3999N - 1000M + 3.379975 \times 10^8$ and $384N + 4160$, respectively. Therefore, the proposed GAN network has the same order of computational complexity as the traditional one [16].

Performance evaluation: We utilize normalized mean square error (NMSE) to measure the similarity between the estimated channel power gain vector $\tilde{\mathbf{h}}$ and the real channel power gain vector $\mathbf{h}$, which is given by

$$\text{NMSE} = \frac{\left\| \mathbf{h} - \tilde{\mathbf{h}} \right\|^2}{\left\| \mathbf{h} \right\|^2}. \tag{8}$$

Fig. 3 shows the heatmaps for estimated channel power gain matrix versus real matrix for different numbers of subchannels (5 and 10 in this figure). It can be seen that the channel power gain predicted by the proposed solution has a good match with the real one.

Fig. 4 shows the NMSE of using the proposed GAN based solution and the traditional GAN in [16]. The proposed GAN based solution has a lower NMSE, namely it can estimate the real channel power gain vector $\mathbf{h}$ more accurately. Moreover, the proposed solution has faster convergence speed. The reasons are twofold: i) An additional cross layer splicing is leveraged to reduce the data information loss in the successive layers of the neural networks and make the proposed GAN model generate samples more effectively; ii) The noise vector and the conditional information vector are extended to increase the richness of information and improve the efficiency of generating accurate samples.

Fig. 5 shows the average NMSE (over 10^4 trials) for the moving vehicle with different accelerations ($a = 5\text{m/s}^2$ and $a = 3\text{m/s}^2$ in this figure). By using the proposed solution, the level of NMSE keeps remarkably low for different motions. As the vehicle's velocity increases, the proposed solution achieves stable performance, i.e, the level of NMSE varies negligibly.

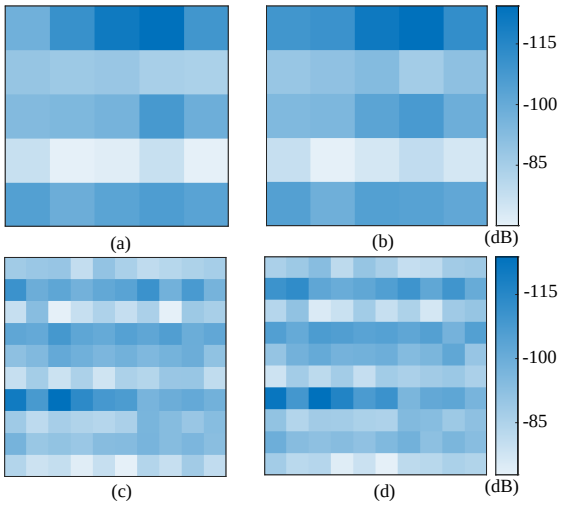

Fig. 3. The heatmaps for the estimated channel power gain matrices versus real matrices with $M = 4$, here, the number of rows represents the number of subchannels with different center frequencies, the number of columns represents the number of vehicles, and the entry in each row represents the level of channel power gain for a subchannel at a vehicle: (a) and (b) are the estimated matrix and the real matrix with $N = 5$, respectively; (c) and (d) are the estimated matrix and the real matrix with $N = 10$, respectively.

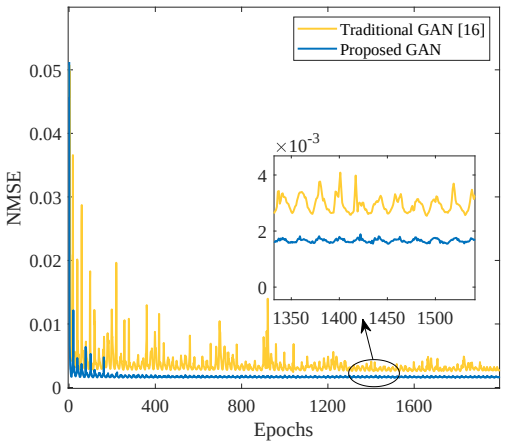

Fig. 4. Performance comparison between traditional GAN and proposed GAN based solutions during the training process.

V. Conclusion and Future Work

A data-driven approach was designed to rapidly estimate the channel power gains in the multi-vehicle THz V2I networks with leaky-wave antennas, which only required single shot channel discovery. By employing vector expansion and twice splicing of the conditional information vector, the proposed GAN based solution improves the efficiency of channel prediction with a fast convergence speed. Simulation results have demonstrated that the proposed GAN based solution can accurately predict the channel power gain and well address the dramatic channel fluctuations due to the high path losses and atmospheric attenuations in the THz frequencies.

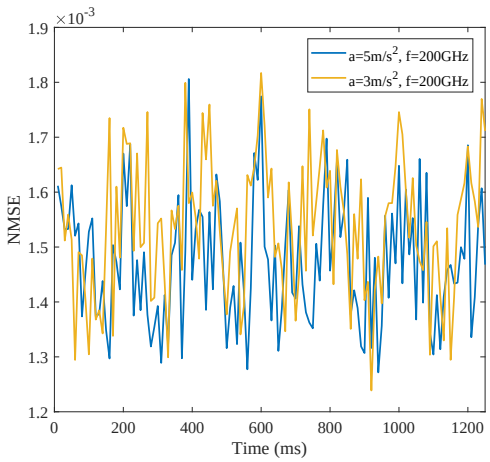

Fig. 5. Performance comparison for the moving vehicle with different accelerations: The minimum communication distance between a vehicle and the RSU is $h = 2$m, the initial states of the considered vehicle include the velocity $v_\circ = 20$m/s, the direction $\varphi_\circ = 4^\circ$ and thus the initial communication distance $d_\circ = h/\sin\theta_\circ = 28.67$m.

While this work has shown the opportunities of using leaky-wave antenna for the V2I channel power gain estimation in the THz frequencies, more research efforts are required to study the dense THz V2I networks, where co-channel interference may have an adverse effect on the estimation performance and needs to be mitigated. In the next-generation intelligent transportation systems (ITS), vehicle platooning will be ubiquitous [21, 22], and efficient THz channel estimation in the platoon systems is another research area. In addition, it is important to design GAN based vehicle positioning.

REFERENCES

[1] T. S. Rappaport *et al.*, "Wireless communications and applications above 100 GHz: Opportunities and challenges for 6G and beyond," *IEEE Access*, vol. 7, pp. 78 729–78 757, June 2019.

[2] H. Sarieddeen, N. Saeed, T. Y. Al-Naffouri, and M.-S. Alouini, "Next generation terahertz communications: A rendezvous of sensing, imaging, and localization," *IEEE Commun. Mag.*, vol. 58, no. 5, pp. 69–75, 2020.

[3] Y. Heng, J. G. Andrews, J. Mo, V. Va, A. Ali, B. L. Ng, and J. C. Zhang, "Six key challenges for beam management in 5.5G and 6G systems," *IEEE Commun. Mag.*, vol. 59, no. 7, pp. 74–79, July 2021.

[4] M. Polese, J. M. Jornet, T. Melodia, and M. Zorzi, "Toward end-to-end, full-stack 6G terahertz networks," *IEEE Commun. Mag.*, vol. 58, no. 11, pp. 48–54, Nov. 2020.

[5] K. Rikkinen, P. Kyöti, M. E. Leinonen, M. Berg, and A. Pärssinen, "THz radio communication: Link budget analysis toward 6G," *IEEE Commun. Mag.*, vol. 58, no. 11, pp. 22–27, Nov. 2020.

[6] Y. Ghasempour, C. Yeh, R. Shrestha, D. Mittleman, and E. Knightly, "Single shot single antenna path discovery in THz networks," in *Proc. 26th MobiCom*, 2020, pp. 1–13.

[7] Z. Lin, L. Wang, B. Tan, and X. Li, "Spatial-spectral terahertz networks," *IEEE Trans. Wireless Commun.*, vol. 21, no. 6, pp. 3881–3892, 2022.

[8] Y. Dong, H. Wang, and Y.-D. Yao, "Channel estimation for one-bit multiuser massive MIMO using conditional GAN," *IEEE Commun. Lett.*, vol. 25, no. 3, pp. 854–858, 2020.

[9] X. Li, A. Alkhateeb, and C. Tepedelenlioglu, "Generative adversarial estimation of channel covariance in vehicular millimeter wave systems," in *Proc. IEEE Asilomar Conf. Signals Syst. Comput.*, Oct 2018, pp. 1572–1576.

[10] P. Jiang, C.-K. Wen, S. Jin, and G. Y. Li, "Dual CNN based channel estimation for MIMO-OFDM systems," *IEEE Trans. Commun.*, vol. 69, no. 9, pp. 5859–5872, Sept. 2021.

[11] M. Gabrié, A. Manoel, C. Luneau, J. Barbier, N. Macris, F. Krzakala, and L. Zdeborová, "Entropy and mutual information in models of deep neural networks," in *NIPS*, 2018, pp. 1821–1831.

[12] I. Goodfellow, J. Pouget-Abadie, M. Mirza, B. Xu, D. Warde-Farley, S. Ozair, A. Courville, and Y. Bengio, "Generative adversarial nets," in *NIPS*, vol. 27, 2014.

[13] H. Ye, L. Liang, G. Y. Li, and B.-H. Juang, "Deep learning-based end-to-end wireless communication systems with conditional GANs as unknown channels," *IEEE Trans. Wireless Commun.*, vol. 19, no. 5, pp. 3133–3143, 2020.

[14] E. Balevi, A. Doshi, A. Jalal, A. Dimakis, and J. G. Andrews, "High dimensional channel estimation using deep generative networks," *IEEE J. Sel. Areas Commun.*, vol. 39, no. 1, pp. 18–30, 2020.

[15] Z. Lin, L. Wang, J. Ding, Y. Xu and B. Tan, "V2I-aided tracking design," *IEEE Int. Conf. Commun. (ICC)*, 2022, pp. 291-296.

[16] M. Mirza and S. Osindero, "Conditional generative adversarial nets," 2014.

[17] A. Sutinjo, M. Okoniewski, and R. H. Johnston, "Radiation from fast and slow traveling waves," *IEEE Antennas Propag. Mag.*, vol. 50, no. 4, pp. 175–181, Aug. 2008.

[18] K. He, X. Zhang, S. Ren, and J. Sun, "Delving deep into rectifiers: Surpassing human-level performance on imagenet classification," in *ICCV*, 2015, pp. 1026–1034.

[19] ITU-R P.676-8 Recommendation, "Attenuation by atmospheric gases," International Telecommunication Union, Geneva, Switzerland, Oct. 2009.

[20] T. K. T. A. P. Molchanov, S. Tyree and J. Kautz, "Pruning convolutional neural networks for resource efficient inference," in *Proc. ICLR*, 2017, pp. 1–17.

[21] T. Zeng, O. Semiari, W. Saad, and M. Bennis, "Joint communication and control for wireless autonomous vehicular platoon systems," *IEEE Trans. Commun.*, vol. 67, no. 11, pp. 7907–7922, Nov. 2019.

[22] L. Wang, Y. Duan, Y. Lai, S. Mu, and X. Li, "V2I-based platooning design with delay awareness," *arXiv preprint arXiv:2012.03243*, Dec. 2020.